The Stability of a Steady Horizontal Shear Front with Uniform Potential Vorticity

ALAIN JOLY
Centre de Recherche en Météorologie Dynamique, Paris
ALAN J. THORPE
Department of Meteorology, University of Reading

(Manuscript received 14 November 1989, in final form 15 May 1990)

ABSTRACT

The stability of the steady two-dimensional horizontal shear front to geostrophic disturbances in the along-front direction is examined within the framework of semi-geostrophic theory. The basic state corresponds to the geostrophic along-front flow at any time during the nonlinear evolution of a two-dimensional Eady wave. The matrix resulting from the stability analysis can be transformed into a weakly nondiagonal form. Its structure shows that the selection of the most unstable along-front wavenumber is independent of the "intensity" of the front. The growth rate is a linear function of this amplitude. The most unstable along-front mode is a modified Eady mode stationary with respect to the front. It draws a fraction of its energy from the shear. For smaller along-front wavelengths, the solution is dominated by propagating modes near the boundaries. These are also baroclinic, with a larger contribution from the basic kinetic energy and much smaller growth rates. It is apparent that the existence of a vorticity maximum at fronts, however large, is not sufficient to produce the observed small scale of frontal waves. Anomalous potential vorticity at the front is necessary to provide a deep zone of large horizontal shear and hence the reduced horizontal scale of waves.

1. Introduction

The idea originally proposed by Bjerknes and Solberg (1922) that midlatitude cyclones result from the release of an instability along the so-called "polar front," appears surprisingly difficult to prove on theoretical grounds. In Solberg (1928) and Orlanski (1968), the structure of the polar front is reduced to two incompressible homogeneous fluids of different speed and density in a rotating frame of reference: this state constitutes the highest degree of idealization of a real front. The dominant mode appears to be a Rayleigh or shear instability of very small scale. Secondary modes of meteorological interest are also found.

The largest scale cyclones are now generally perceived as *baroclinic waves,* releasing the instability of jet-flows. Even normal modes of one-dimensional vertically sheared flows have a remarkable number of features in common with observed cyclones, in terms of scale or structure. However, this quasi-geostrophic theory of cyclogenesis, steming from the work of Eady (1949) and Charney (1947) predicts stability for waves with wavelength less than 1000 km. Such waves are, however, observed to grow, on occasion, in the frontal regions resulting from the nonlinear growth of the primary baroclinic waves.

The recent work of Moore and Peltier (1987), Schär and Davies (1990), and Joly and Thorpe (1990) have considered these issues from a new perspective. The basic state considered in these studies arises from the semi-geostrophic model of front. The source of the instability differs in these papers. Joly and Thorpe prove the proposal formulated by Thorpe and Emanuel (1985) that a potential vorticity anomaly of small transverse scale produced by condensation is necessary to significantly destabilize fronts on the 1000 km wavelength. Schär and Davies (1990) considered a simplified version of the same idea. Both studies remain within the framework of semi-geostrophic theory.

The approach of Moore and Peltier differs in that they use the linearised primitive equations. Exploring the stability of the steady deformation front in uniform potential vorticity flow, they found two sets of normal modes: a modified Eady mode with wavelength between 3000 km and 5000 km, and what appeared as a new mode, with wavelength about 1000 km. This cyclone scale mode had a smaller growth rate than the baroclinic mode, with an *e*-folding time of one day. However, the mechanism for the growth of this mode remains unclear.

Here the stability of the two-dimensional horizontal shear front is analyzed using semi-geostrophic theory. This basic state is simple enough so that, although nonseparable, it can be transformed analytically into an eigenvalue problem. The solution of that eigenvalue problem is found using a numerical method.

The structure of the front formed by horizontal shear in a simple growing baroclinic wave is now well known. Regions of large gradients in potential temperature and

Corresponding author address: Dr. Alain Joly, Centre de Recherche en Météorologie Dynamique, 2 avenue Rapp, F-75340 Paris cedex 7, France.

along-front wind are confined to the upper and lower boundaries, as there the fluid cannot escape the frontogenetic effect of shear by moving vertically. Its main characteristics are boundary-jets, symmetric with respect to the front, with large vertical shear implying a large anomaly in potential temperature. Although highly idealized, it appears more realistic than the two-fluid problem of earlier studies on frontal stability (Fig. 1).

The functional form of the fields is very complicated, and the resulting stability problem appears hopelessly nonseparable. However, the nonlinear aspect of the solution results entirely from the ageostrophic displacement of air parcels in the jets. The semi-geostrophic framework implies a change of horizontal coordinates. In the transformed space, ageostrophic displacements are implicit (but not neglected, as in quasi-geostrophic theory), and the solution becomes a simple wave. The resulting equations remain nonseparable, but become more directly tractable.

2. The stability problem

Here we consider a horizontally periodic domain (the domain width shall be denoted L, the corresponding wavenumber being $k = 2\pi/L$) on an f-plane bounded vertically by free surfaces where pressure is assumed constant at $z^* = \pm h$. z^* is the coordinate introduced by Hoskins and Bretherton (1972): $z^* = C_p H_s / R_a [1 - (p/p_{00})^{R_a/C_p}]$, with H_s the scale height. The potential vorticity is a constant. A Boussinesq-type approximation is made, the changes of density r with height z^* are neglected; i.e., $r = \rho_0$ everywhere. It is useful to rescale potential vorticity as an equivalent buoyancy frequency:

$$\mathcal{N}^2 = \frac{g}{\theta_0} \frac{\rho_0 P_{00}}{f} . \tag{1}$$

The mathematical simplification obtained by using the geostrophic momentum approximation is limited because advection by ageostrophic velocities is pre-

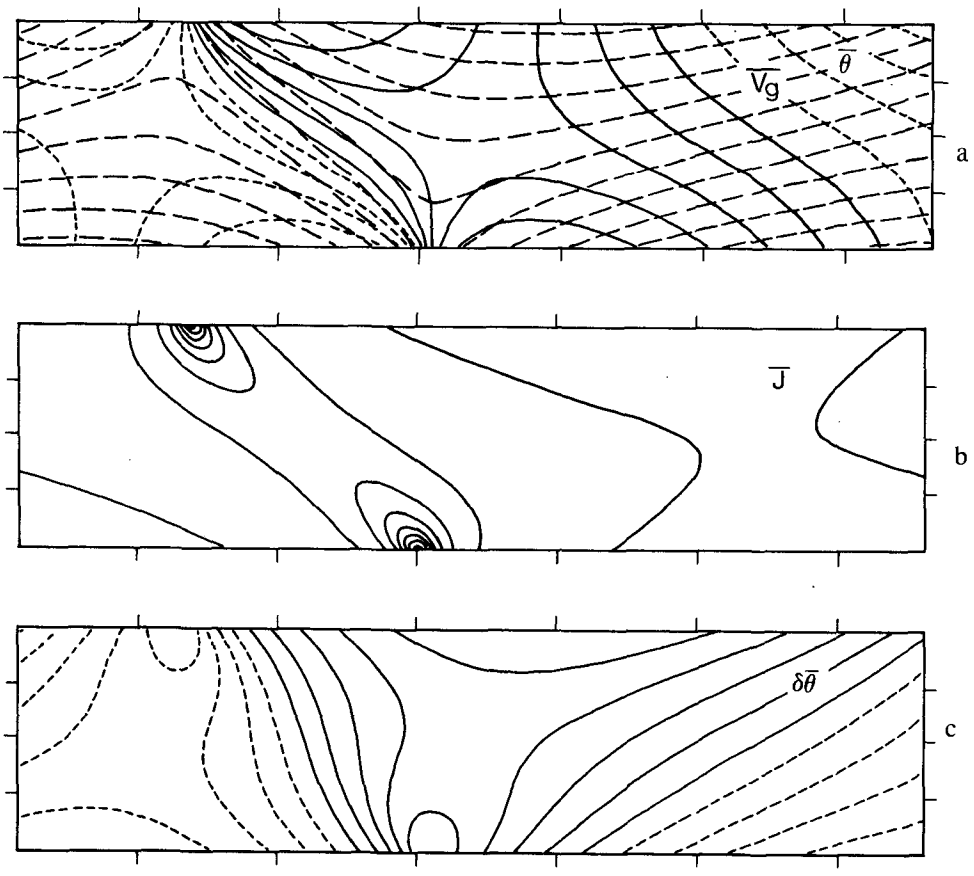

FIG. 1. Vertical cross sections of a two-dimensional Eady wave in the nonlinear regime, showing an idealized mature cold front in a dry atmosphere. Tick marks horizontally every 500 km, 2 km vertically. (a) Solid and dotted lines, long-front geostrophic wind $\overline{V_g}$, contour interval 9 m s^{-1}, negative lines dotted. Dashed lines, potential temperature $\bar{\theta}$, contour interval 5 K; (b) Nondimensional absolute vorticity $\bar{J}$ (also the jacobian of the change to geostrophic coordinates), $\bar{\zeta}_a/f$, contour interval 0.7, maximum value 8.3; (c) Potential temperature departure from the hydrostatic vertical profile at rest $\overline{\delta\theta} = \bar{\theta} - \theta(Z)$, contour interval 3 K, negative contours dashed.

served. This is crucial in the formation of frontal zones. However, this process becomes mathematically implicit, thus removing a large part of the nonlinearity, if a change of horizontal coordinates is made (Hoskins and Bretherton 1972; Hoskins 1975). The geostrophic coordinates are:

$$X = x + v_g/f, \quad Y = y - u_g/f, \quad Z = z^* \qquad (2)$$

where x is the across-front direction, y the along-front, and (u_g, v_g) the geostrophic wind. Displacements in transformed space are geostrophic.

The horizontal shear front results from the nonlinear growth of a two-dimensional Eady wave, a process well described by the semi-geostrophic theory based on the previous assumptions and ideas. Here we examine the stability of this front to along-front perturbations assuming that the frontogenesis, associated with $\overline{U_z}$, has been removed. Only an along-front geostrophic flow remains: the steady basic state whose stability is examined below.

In geostrophic space, the front within its parent baroclinic wave is described by the following equations:

$$\bar{\theta} = \left(\theta_0 + \frac{\theta_0}{g}\mathcal{N}^2 h\right) + \frac{\theta_0}{g}\mathcal{N}^2 Z + \frac{\theta_0}{g}\frac{\phi_0}{H_k} \times \left(R\cosh\frac{Z}{H_k}\cos kX + I\sinh\frac{Z}{H_k}\sin kX\right)$$

$$\overline{V_g} = \frac{\phi_0 k}{f}\left(-R\sinh\frac{Z}{H_k}\sin kX + I\cosh\frac{Z}{H_k}\cos kX\right)$$

$$\frac{1}{\bar{J}} = 1 + \frac{\phi_0 k^2}{f^2} \times \left(R\sinh\frac{Z}{H_k}\cos kX + I\cosh\frac{Z}{H_k}\sin kX\right). \qquad (3)$$

They give the distribution of potential temperature $\bar{\theta}$, geostrophic along-front wind $\overline{V_g}$ and the nondimensional absolute vorticity $\bar{J} = \overline{\zeta_a}/f$. The latter is also the Jacobian of the transform to geostrophic space. The fundamental constants are:

$$H_k = \frac{f}{\mathcal{N}k}$$

which is the Rossby "depth" of the Eady wave; and

$$R = \frac{\sqrt{\coth\chi - \chi}}{\cosh\chi}$$

$$I = \frac{\sqrt{\chi - \tanh\chi}}{\sinh\chi}$$

which are its amplitude constants, where $\chi = h/H_k$ is the nondimensional horizontal wavenumber of the wave. ϕ_0 is the finite amplitude of the steady state wave.

Equations (3) represent the along-front flow in a normal mode of the Eady basic state at any given time. For this mode to be unstable requires $0 < \chi < \chi_c$ where $\chi_c \approx 1.2$. The most unstable Eady mode is for $\chi = \chi_u \approx 0.80$; and provided ϕ_0 is redefined, the amplitude factors can be simplified to:

$$R = 1/\sinh\chi_u \quad \text{and} \quad I = 1/\cosh\chi_u.$$

There is another bound on the range of parameters: the solution, which can be constructed for any value ϕ_0 in geostrophic space, must be taken before frontal collapse in physical space. Furthermore, the geostrophic momentum approximation breaks down because of turbulence when $1/\bar{J}$ becomes less than 0.1 (Hoskins 1982). Within these limits χ and ϕ_0 are arbitrary.

A three-dimensional infinitesimal perturbation is superimposed on this flow, with the assumption that it also has uniform potential vorticity. The equations governing the evolution of such a perturbation using semi-geostrophic theory were derived by Hoskins (1976).

The geostrophic part of the solution is completely determined by a potential $\Phi' = \phi' + \overline{V_g}v_g'$, where ϕ' is the geopotential and the overbar denotes the basic front. Perturbation parameters are primed. The potential Φ, defined as $\Phi = \phi + 1/2(u_g^2 + v_g^2)$, is a "streamfunction" of the geostrophic component of the flow:

$$\left(fU_g', fV_g', \frac{g}{\theta_0}\theta'\right) = \left(-\frac{\partial\Phi'}{\partial Y}, \frac{\partial\Phi'}{\partial X}, \frac{\partial\Phi'}{\partial Z}\right). \qquad (4)$$

The potential Φ is related to potential vorticity in the interior domain as, by definition $\rho_0 P_{00} = fJ\partial\theta/\partial Z$. If the perturbation potential vorticity P' is initially zero, it will remain so. Linearized, this equation is then reduced to Laplace form:

$$\frac{\partial^2\Phi'}{\partial X^2} + \frac{1}{\bar{J}}\frac{\partial^2\Phi'}{\partial Y^2} + \frac{f^2}{\mathcal{N}^2}\frac{\partial^2\Phi'}{\partial Z^2} = 0. \qquad (5)$$

Here the weight $\bar{J}$ on the Y-derivative is set to unity, as in Hoskins' original derivation. The independent, fully two-dimensional method developed by Joly and Thorpe (1990) for solving more elaborate versions of Eq. (5), including the Jacobian weighting and nonuniform potential vorticity, was used here to test this assumption. It was found that with uniform potential vorticity, results are not affected. Further comments about its impact with nonuniform potential vorticity can be found in section 4.6 of Joly and Thorpe (1990).

The linearised equations for θ on the surface and top boundaries, with conditions $w' = 0$ at $Z = \pm h$, are:

$$\left(\frac{\partial}{\partial T} + \overline{V_g}\frac{\partial}{\partial Y}\right)\theta' = -U_g'\frac{\partial\bar{\theta}}{\partial X} \quad \text{at} \quad Z = \pm h. \qquad (6)$$

As the basic state does not depend on T or Y, a solution in the form of an independent normal mode is:

$$\Phi' = \hat{\phi}(X, Z)e^{i\ell Y}e^{\sigma T} \qquad (7)$$

where ℓ is the along-front wavenumber of the perturbation, and σ its growth rate. Our primary goal is the functional form of the dispersion relation $\sigma(\ell)$, and

the way this relation depends on the basic state. The Fourier transform of Eq. (5) and Eq. (6) along Y and the Laplace transform in time yield is:

$$\frac{\partial^2\hat{\phi}}{\partial X^2} - \rho^2\hat{\phi} + \frac{f^2}{\mathcal{N}^2}\frac{\partial^2\hat{\phi}}{\partial Z^2} = 0$$

$$(\sigma + i\ell\overline{V_g})\frac{\partial\hat{\phi}}{\partial Z} - i\ell\frac{\partial\overline{V_g}}{\partial Z}\hat{\phi} = 0 \quad \text{on} \quad Z = \pm h$$

after making use of the thermal wind equation to substitute for $\partial\bar{\theta}/\partial X$ and the definition of $\theta'(\Phi')$ and $U_g'(\Phi')$. As there is a periodic domain in X, $\hat{\phi}(X)$ can be expressed as a Fourier series:

$$\hat{\phi}(X, Z) = \sum_{m=-\infty}^{+\infty} \phi_m(Z)e^{imkX}. \tag{8}$$

(Note that since $\hat{\phi}(X, Z)$ may be complex then, if ℓ is not zero, ϕ_0 is not necessarily zero, and ϕ_{-m} is not necessarily the complex conjugate of ϕ_m.) From (3), the basic state on the boundaries is given by:

$$\overline{V_g}(\pm h) = \mp V_1 \sin kX + V_2 \cos kX$$

$$\frac{\partial\overline{V_g}}{\partial Z}(\pm h) = \frac{V_3}{H_k}\sin kX \pm \frac{V_4}{H_k}\cos kX$$

with

$$V_3 = -\frac{\phi_0 k}{f}\sqrt{\coth\chi - \chi} \quad V_1 = -V_3\tanh\chi$$

$$V_4 = \frac{\phi_0 k}{f}\sqrt{\chi - \tanh\chi} \quad V_2 = V_4\coth\chi. \tag{9}$$

In order to Fourier transform in X, the equations are multiplied by e^{-inkX}, integrated over the domain, and $\hat{\phi}(X)$ is expanded in series of ϕ_m following (8). In the interior equation, all integrals are zero except when $n = m$, thus:

$$\frac{d^2\phi_m}{dZ^2} - \frac{\phi_m}{H_m^2} = 0 \text{ with } H_m = \frac{f}{\mathcal{N}\sqrt{k^2m^2 + \ell^2}}. \tag{10}$$

Substituting into the boundary equations, we obtain:

$$\lambda\frac{d\phi_m}{dZ} + \frac{\ell}{2}\left[(V_2 \mp iV_1)\frac{d\phi_{m+1}}{dZ} + (V_2 \pm iV_1)\frac{d\phi_{m-1}}{dZ} - (\pm V_4 + iV_3)\frac{\phi_{m+1}}{H_k} - (\pm V_4 - iV_3)\frac{\phi_{m-1}}{H_k}\right] = 0 \quad \text{on} \quad Z = \pm h \tag{11}$$

where $\lambda = -i\sigma$.

Because of the simple form of the frontal solution, the nonseparability involves only adjacent harmonics on the boundaries. As the interior equation has been diagonalized in the process, we deduce the functional form $\phi_m(Z)$:

$$\phi_m(Z) = A_m\cosh\frac{Z}{H_m} + B_m\sinh\frac{Z}{H_m} \tag{12}$$

where A_m and B_m are complex constants having the dimensions of a potential. Upon substitution of this solution into the boundary equations (11), the stability problem is transformed into a standard algebraic eigenvalue problem, although not immediately diagonal. The solution can be determined up to any finite order of precision M. Assuming that ϕ_{M+1}, ϕ_{-M-1}, ϕ_{M+2}, ϕ_{-M-2}, etc. are zero, the ensemble of $2M + 1$ systems can be written as

$$\lambda\mathbf{a} = -\ell\cdot\mathbf{D}\cdot\mathbf{a} \tag{13}$$

where $\mathbf{a}^T = (A_{-M}, B_{-M}, \cdots, A_m, B_m, \cdots, A_M, B_M)$ and $\mathbf{D}$ is a complex matrix of order $4M + 2$. The analytical expression of $\mathbf{D}$ is given in the Appendix. All that is needed is a standard routine computing its eigenvalues and eigenvectors.

3. Growth rates curves

a. Properties of the general solution

In the limit of small wavenumbers ℓ, all terms of $\ell\mathbf{D}$ behave like ℓ except the coefficients of the equation for A_0, which are equivalent to ℓ^{-1}. This particular limit can thus be analyzed with a low order characteristic polynomial in m (Joly 1989). As expected from Eq. (13), σ becomes continuously zero as l decreases.

In the limit of large wavenumbers ℓ, $\mathbf{D}$ becomes a Hermitian matrix. Its eigenvalues λ are thus real, so the growth rate $\sigma = -i\lambda$ is purely imaginary: the flow is stable. This result holds at least for any finite order of truncation M.

Probably the most interesting property of the eigenvalue problem (14) stems from the form of the coefficients in $\mathbf{D}$. They contain scales that can be nondimensionalized by the Rossby radius $\mathcal{N}h/f$. The only dimensional factors are V_1 to V_4 in (9). They contain all the information about the "strength" of the front in that they are proportional to the amplitude of the Eady wave ϕ_0. Now nondimensionalize V_1 to V_4 by $\phi_0 k/f$. The eigenvalue problem can then be rewritten:

$$\tilde{\sigma}\mathbf{a} = -i\tilde{\ell}\tilde{\mathbf{D}}\cdot\mathbf{a}$$

where $\tilde{\sigma} = \sigma(\mathcal{N}h/\phi_0 k)$; $\tilde{\ell} = \ell(\mathcal{N}h/f)$; and $\mathbf{D}$ contains only nondimensional numbers, functions of χ, χ_m, and ratios H_m/H_n and H_m/H_k.

Therefore, the Rossby radius of deformation $\mathcal{N}h/f$ is the unit of length, and the relevant unit of time appears to be $\mathcal{N}h/(\phi_0 k)$. The point is that $\tilde{\ell}$ and $\tilde{\mathbf{D}}$ are now *independent* of ϕ_0. Thus, once the potential vorticity $\mathcal{N}$ and the geometry (f, h and k) are known, the dimensional properties of $\sigma(\ell)$, such as the wavenumber of maximum growth or transition to stability, will not depend on the amplitude of the front, it will not depend on how near it is to frontal collapse. The reduction of horizontal scale of the front does not affect

this aspect of the solution. It shows, however, that the growth rate σ is a linear function of the amplitude of the Eady wave ϕ_0, at all scales ℓ.

b. *The long-wave modes*

The series were truncated at order $M = 21$. The martrix **D** is of order 86. Eigenvalues were computed with the NAGLIB routine for general complex matrices. For several values of the across-front wavenumber χ, calculations were repeated with several resolutions to check the stability of the procedure. When needed, the following constants were used to recover dimensional values: $f = 10^{-4}$ s^{-1}, $H_s = 8000$ m, $\mathcal{N} = 1.04$ 10^{-2} s^{-1} corresponding to $P_{00} = 0.3$ PVU (1 PVU $= 10^{-6}$ m^2 K s^{-1} kg^{-1}), and $h = 4000$ m.

Figure 2 shows these modes as a function of both wavenumbers. These modes have zero frequency in this reference frame; i.e., $\sigma_i = -\ell c_i = 0$, so the mode has a phase speed equal to the mean flow $\overline{V_g}(0)$. They are dominant up to the thinning point. The valid solution beyond this point is discussed below. For a given wavelength of the parent baroclinic wave, the long-wave growth rate curves are as in an Eady-type problem, with a single well-defined maximum.

These modes appear possible only at large wavelengths. A remarkable property of the solution is apparent from the figure: these modes exist only if the along-front wavenumber ℓ of the perturbation is *smaller* than the parent wave wavenumber; i.e., $\sigma_i = 0$ occur for $\ell \leqslant k$.

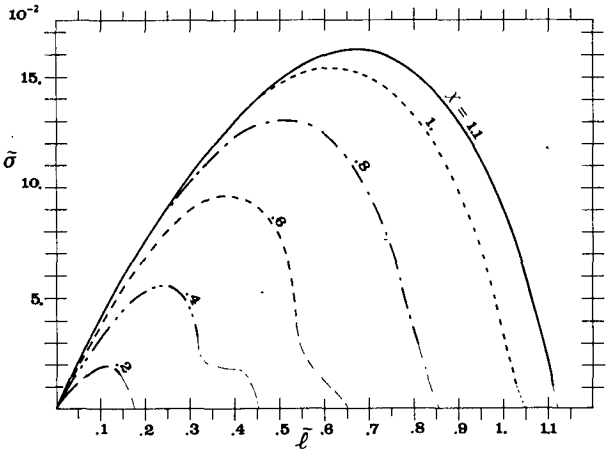

FIG. 2. Nondimensional real part of the growth rate of a normal mode perturbation superimposed on the steady shear front as a function of the across-front wavenumber of the parent baroclinic wave χ and the nondimensional along-front wavenumber of the perturbation $\tilde{\ell}$. The curves pertain to the zero frequency modes. Taken together, the curves, resulting from a continuous change of the parameters ($\tilde{\ell}$, χ), form a well-defined two-dimensional surface. The limit beyond which smaller-scale modes have larger growth rates is suggested by a change in the thickness of the lines. Below this line, growth rates were recovered empirically among the 86 possible values delivered by each calculation for a given $\tilde{\ell}$.

Since the range of unstable wavenumbers increases with increasing χ, the most unstable wavenumber in the along-front direction also increases. It increases essentially linearly from $\tilde{\ell} = 0.125$ for $\chi = 0.2$ to $\tilde{\ell} = 0.675$ for $\chi = 1.1$. Recall that the wavenumbers are intrinsic solutions of the stability problem; they are independent of the "intensity" of the front. For a small scale Eady wave with $\chi = 1.1$, which is an across-front wavelength of about 2400 km, the most unstable along-front perturbation has a wavelength of more than 3800 km.

The maximum growth rate $\tilde{\sigma}$ also increases quasi-linearly with the Eady wavenumber χ. The dimensional growth rate can be written

$$\sigma = \frac{\phi_0 f}{(\mathcal{N}h)^2}\chi\tilde{\sigma}.$$

This expression shows that if $\tilde{\sigma}$ is a linear function of χ, the dimensional growth rate will increase as χ^2. For example, with $\phi_0 = 2052$ J kg^{-1}, the e-folding time is shorter than a day for χ larger than 0.8 and reaches 0.5 day for $\chi = 1.1$.

Despite its large growth rate, this kind of solution does not offer a suitable explanation for frontal waves: the horizontal scales involved are much too long.

c. *The smaller scale modes*

Beyond an approximate limit, $\tilde{\ell} = \chi$, unstable modes appear in conjugate pairs (that is, with opposite phase speeds with respect to the front). We now find whether secondary maxima in growth rate are allowed on the 1000 km scale.

The growth rate curve for these modes is depicted by Fig. 3. Only one significant maximum occurs near the wavenumber at which the conjugate modes supersede the stationary mode. The maximum value occurs at $\chi = 0.6$. The growth rate is four times smaller than the absolute maximum of the stationary mode family. The corresponding dimensional value (3.2 10^{-6} s^{-1}) is an e-folding time of about 4 days. Although unstable, modes on the 1000 km scale have typical e-folding times of a fortnight.

A final property of interest of the eigenvalues of (13) is shown by the absolute value of the nondimensional phase-speed relative to the midlevel flow. Except for very small χ, it reaches an asymptotic limit of about 0.6 units, quasi-independent of the parent wave basic wavenumber χ.

It has been shown that the instability of a finite amplitude Eady wave differs from that of a constant shear flow in having a separate short-wave mode. The mechanism of instability of this mode is the same as that described by Schär and Davies (1990) for a different, but still uniform potential vorticity, basic flow. This has been called "the warm-band" mechanism; but more generally, for uniform potential vorticity, it relies on a local extremum of temperature at the surface.

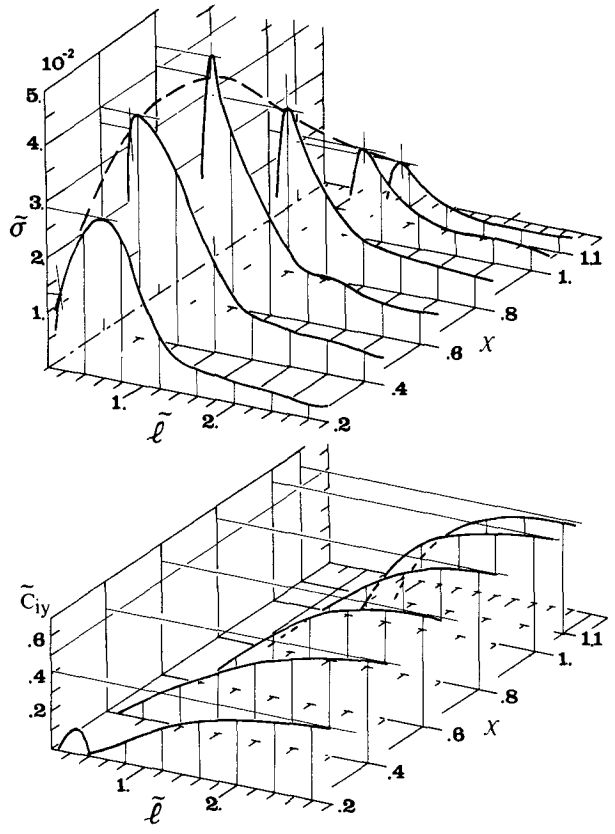

FIG. 3. Upper panel as in Fig. 2, but at larger along-front wavenumbers. Above the heavy dotted line, zero frequency modes dominate. Lower panel is the nondimensional along-front phase speed of the modes as function of the same wavenumbers as above.

Such an extremum is produced in an Eady wave where the warmest air in the cyclone is located near the cold front. To this extent the Eady wave basic state used here is a realistic representation of an observed frontal region. These modes are controlled by geostrophic dynamics. The growth rates we obtain using the finite amplitude Eady wave as the basic state are, however, extremely small. It is worth noting that the short-wave mode found by Moore and Peltier (1987) cannot rely on this mechanism for instability as they used the so-called Hoskins–Bretherton deformation front as the basic flow; this does not contain a temperature extremum.

4. The nature of the normal modes

The structure of one of the long-wave modes is examined in detail in order to characterise the dominant instability. The basic flow here is substantially different from the constant shear of the original Eady problem and so it is of interest to look at the structure of these three-dimensional modes. The most unstable mode for $k = 1.94\ 10^{-6}\ \mathrm{m}^{-1}$, that is $\chi = 0.8$, has an along-front wavelength of about 5 200 km. From the eigenvector **a**, $\phi'(X, Y, Z)$ is computed as well as the geostrophic components of the flow (including θ') by making use of the functional form of the normal mode (7) and (12). The Appendix shows how the Fourier components of the vertical velocity can be recovered from θ' and Φ'.

A cross section of the flow along the front, on the cold side, induced by the mode alone, is displayed in Fig. 4. The mode is deep and the flow across the plane, U'_g, possesses a distinct tilt with height, whereas the potential temperature anomaly has moderate opposite tilt. Also noticeable is that the vertical circulation is thermally direct. All these are characteristic features of a classical baroclinic wave. In this three-dimensional wave, there is also a geostrophic circulation in the Y–Z plane that derives its energy from the large shear present at the front. A horizontal section reveals a characteristic wavenumber 2 pattern of the mode in the cross-front direction (Fig. 5). The picture has been drawn in physical space, the transformation from geostrophic to physical space being defined by the basic state alone, in order to be consistent with linear theory. The amplitude ϕ_0 is the same as in Fig. 1, namely $\phi_0 = 2917\ \mathrm{J\ kg}^{-1}$. The amplitude of the potential temperature wave is 15 K, the maximum vorticity $8.3f$.

The maximum amplitude is separated in two quasi-symmetric kernels, nearly out of phase with one another on each side of the front. The frontal region itself is avoided. A possible interpretation is that the shear is too strong to allow organization of the mode. However, as shown by the midtroposphere vertical velocity, only one of these two kernels is really active: the one on the cold side "north" of the front. As the front slopes in the same direction, the active part of the perturbation seems strongly aided by the geostrophic frontal structure.

The linear three-dimensional Eady mode having the same wavenumbers can be compared to this frontal large scale mode. Strong similarities are observed. In geostrophic space, the horizontal structures differ mostly by their tilt: 45° for the Eady mode (giving a wavenumber 2 impression), and 20° for the frontal mode. In both, lows are combined with a warm anomaly of potential temperature and with ascent. The reversed phase change of θ' is enhanced in the classical solution. While the phase tilts of an Eady mode are horizontally uniform (the eigenmode depends on Z only), they are reversed in the frontal wave mode depending on the side of the front (the frontal eigenvector is a function of X and Z).

The frontal wave has two obvious energy sources: the kinetic energy in the frontal jets, with large shear to enhance conversion, and the equally large temperature gradient, implying a source of potential energy. Margules (1905) thought that the atmospheric waves were mostly driven by the latter, but when Solberg (1928) attempted to study the two-fluid problem, he found a larger contribution from the basic state kinetic

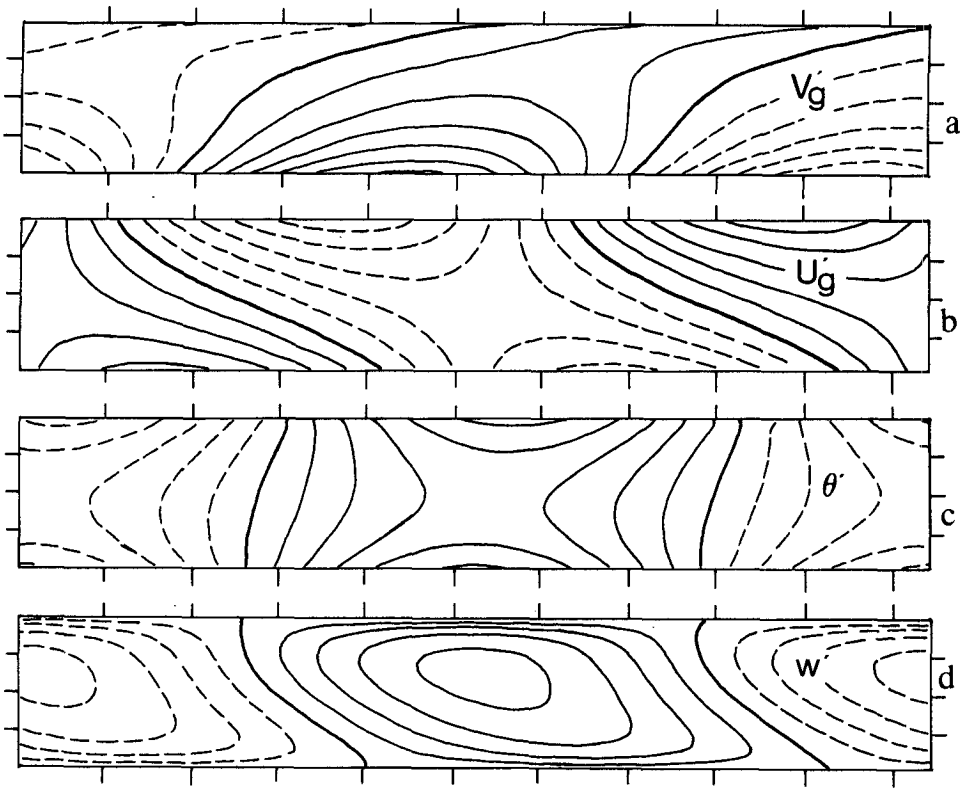

FIG. 4. Vertical cross section of the flow associated with the most unstable normal mode for $k = 1.9\ 10^{-6}$ m^{-1} ($\chi = 0.8$) in the along-front Y direction. The picture is drawn in geostrophic space (X = constant) corresponding to the location of the surface front of Fig. 1. In physical space, this section is slanted. The basic state is not superimposed. Tick marks are set every 500 km horizontally, every 2 km vertically. Negative contours are dashed, the zero line is thickened. (a) Geostrophic wind V'_g in the plane; (b) Geostrophic wind U'_g accross the plane; (c) Potential temperature perturbation θ'; (d) Vertical velocity w'. Contour intervals are arbitrary but consistent with one another. If the interval in (a) is one unit (1 m s^{-1}), then it is the same in (b), 0.6 K in (c), and 0.2 cm s^{-1} in (d).

energy. Baroclinic instability theory justified the early intuition of Margules.

In the present work, energetics are an instance where the use of a transformed space is not an advantage. At the level of linear theory, however, the energy equations in transformed space can be used (Joly and Thorpe 1990).

A mode for which the Reynolds stress term is zero and the energy source is the mean potential energy will be called a "baroclinic mode." Conversely, a mode with zero horizontal heat flux conversion, growing solely from the main kinetic energy will be named a "barotropic mode." The internal conversion can have both signs: it is positive in "pure" baroclinic waves and negative in barotropic instability in a stratified fluid.

The energy cycle of the most unstable mode growing in a steady horizontal shear front is shown in Fig. 6. It confirms the primarily baroclinic nature of the large scale frontal wave, with, however, a significant contribution of the kinetic energy that is absent from the Eady problem.

The scales of a given mode as compared to the dimensions of the basic state are shown by the weighted along-front mean wave correlations in the plane of symmetry (X, Z) (Fig. 7). The wavenumber 2 pattern is present as well as the "deep" nature of the mode. The asymmetry between the two maxima becomes very clear. The baroclinic cycle activates the wave "north" or coldward of the front, closely following the frontal shape itself. However, the "southern" kernel depends mostly on the barotropic mechanism. Apart from this, the main part of the unstable wave is directly linked to the front itself.

It has been argued previously that the bimodal structure of the frontal wave mode is due to the large shear at the front. The energy correlations contradict this idea. The front, defined as the zone of maximum vorticity, is the most active part of the wave. The "inactive" region corresponds to zones of zero baroclinicity: the frontal wave avoids those parts of the flow where conversion is impossible for lack of any source. It is only at the boundaries that the front and the extrema of potential temperature anomaly are near one another.

The short-wave modes are of similar structure, but, as the along-front wavenumber ℓ increases, the max-

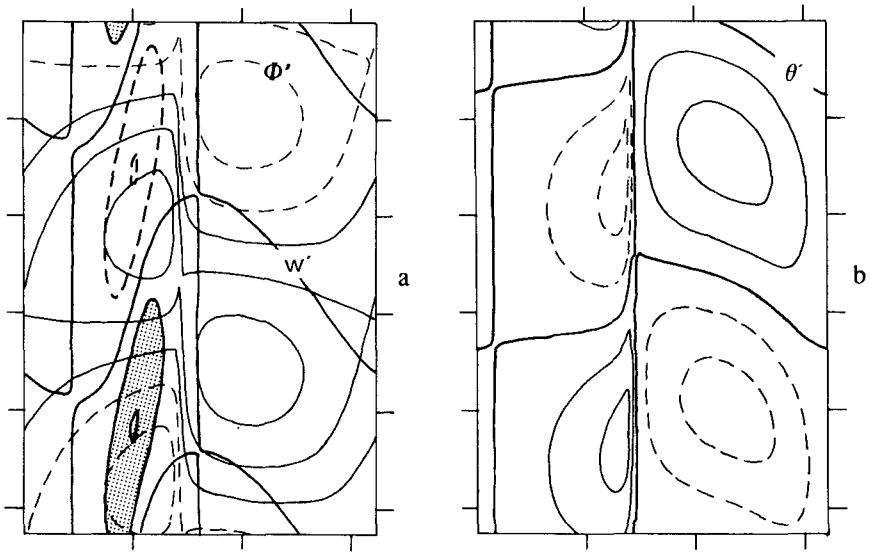

FIG. 5. Horizontal cross section of the flow associated with the mode of Fig. 4, in the physical space defined by the basic state shown by Fig. 1. The latter is not superimposed. Tick marks are set every 1000 km. Negative contours are dashed or dotted. (a) Thin contours, geostrophic potential perturbation Φ' near the surface (Z = 410 m), contour interval 180 J kg^{-1}. Thick lines, vertical velocity at midlevel (Z = 4108 m), contour interval 0.4 cm s^{-1}, positive values larger than 0.4 cm s^{-1} are shaded; (b) Potential temperature perturbation θ' near the surface (Z = 410 m), contour interval 1.2 K.

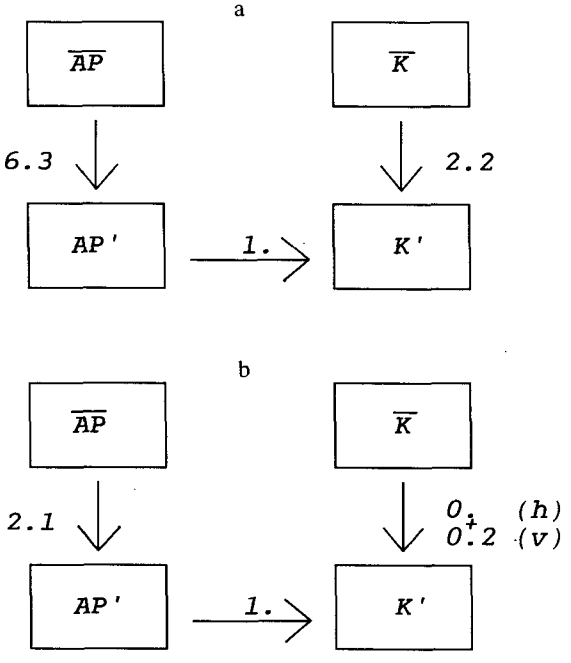

FIG. 6. Energy box diagram, showing the rates of conversions as well as their signs, normalized by the internal conversion based on the correlation $\langle w'\theta' \rangle$. The quantity AP stands for a reservoir of available potential energy, K for kinetic energy. The overbar denotes a basic state property, the prime a perturbation quantity. The conversion from $\overline{AP}$ to AP′ is based on $\langle \overline{\partial_x \theta} u'_g \theta' \rangle$, the conversion from $\bar{K}$ to K' is dominated by $\langle \overline{\partial_x V_g} u'_g v'_g \rangle$. (a) the conversions for the most unstable mode of Fig. 2 for χ = 0.8; (b) the conversions for the three-dimensional Eady mode having the same wavenumbers as in (a) for reference where h refers to the horizontal Reynolds stress and v to the vertical Reynolds stress terms.

imum amplitude is confined to shallower regions near the boundaries. Considering the smallness of the growth rates, a more detailed analysis is not needed here. The introduction of friction near the boundary layer would ruin their weak and shallow energy converting structures.

5. Conclusions

Examples of a basic flow whose stability can be studied analytically are hard to find. Generally, the flow has to be described by constant coefficients, or at most, one-dimensional functions. A realistic frontal zone, with its localized regions of large gradients, seems beyond the reach of simple techniques. However, a large part of the complexity of the frontal flow is removed by the transformation to geostrophic coordinates. It turns out that the horizontal shear front solution, resulting from the growth into the nonlinear regime of a two-dimensional unstable Eady wave can thus be described by a simple sinusoidal function. The basic state remains two-dimensional, and one single harmonic is enough to represent the front within the parent baroclinic wave. Another simplification is the constancy of the potential vorticity. With these assumptions, the normal mode instability of a steady two-dimensional horizontal shear front can, in essense, be described analytically. The simple form of the interior equations allows the problem to be reduced to the two horizontal boundary conditions. This is mathematically equivalent to removing the vertical dimension. However, as the basic state *is* two-dimensional, the transformed eigenvalue problem remain nondiagonal.

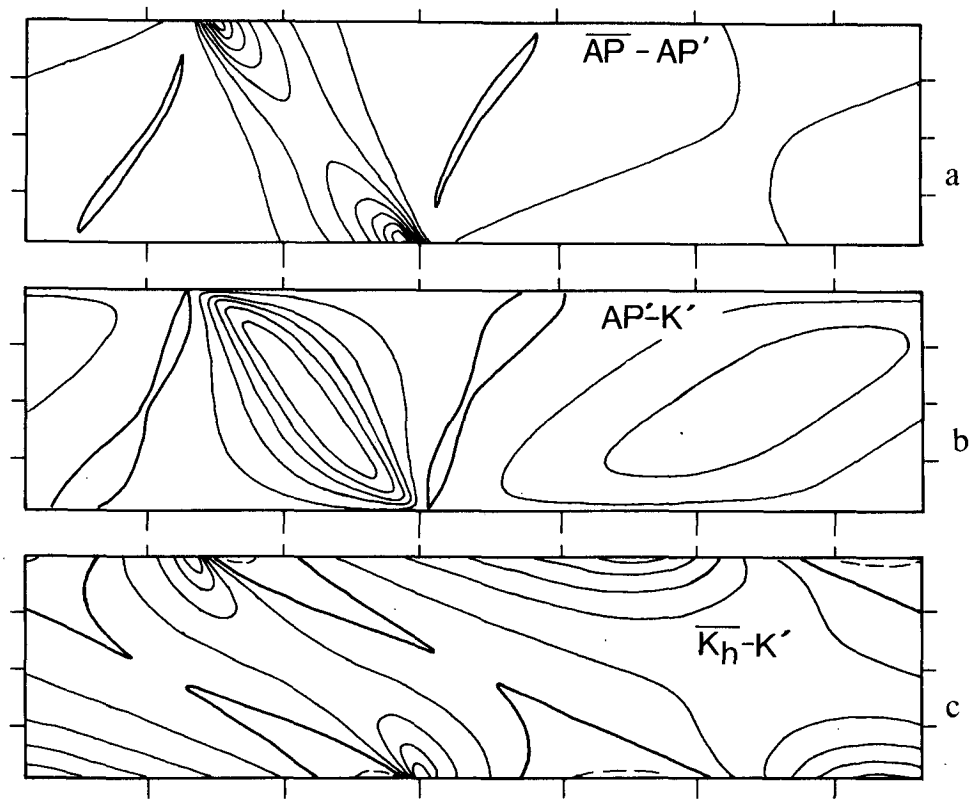

FIG. 7. Energy conversions over one wavelength in Y in the flow induced by the most unstable normal mode of Fig. 2 for $\chi = 0.8$ in a vertical cross section in a (x, z^*) plane, in the physical space defined by the basic state shown by Fig. 1. Symbols as in Fig. 6. Ticks are set every 500 km horizontally, every 2 km vertically. Zero contour are thickened, negative contour dashed. (a) Potential energy conversion, contour interval of 1 unit (1 unit is 10^{-4} J kg^{-1} s^{-1} in SI); (b) Internal conversion, contour interval 0.16 unit; (c) Kinetic energy conversion, contour interval 0.4 unit.

The solution and properties studied here apply to all two-dimensional basic states with uniform potential vorticity that can be described in transformed space by one harmonic only. It includes the jet flows considered by Hoskins and West (1979). The present conclusions are therefore pertinent for synoptic scale meteorology: for instance, the wavenumber selection is, unlike the growth rate, independent of the maximum jet speed.

Concerning the small-scale mode typical of frontal waves, we find that they exist in a balanced model with uniform potential vorticity with a horizontal scale along the front of about 1000 km. The basic flow in which these waves develop is that flow produced at any stage during the development of a two-dimensional Eady wave. Although this flow differs from that discussed by Schär and Davies (1990) the necessary condition for the instability is the same; namely that $\partial\bar{\theta}/\partial X$ $(Z = +h)$ or $\partial\bar{\theta}/\partial X$ $(Z = -h)$ have both signs on either of the vertical boundaries. An important result of this paper is that however large the horizontal shear is in the parent Eady-type wave, with uniform potential vorticity the most unstable frontal wave has an unrealistically large scale to account for the observed phenomenon. This result applies to any such basic flow that can be described in the geostrophic momentum coordinate space by one harmonic; it does not apply to the flow used by Schär and Davies (1990) because of the asymmetry in the surface potential temperature distribution. Also, in the work of Moore and Peltier (1987), a uniform potential vorticity flow appears to have a short-wave mode even without the instability mechanism highlighted here and in Schär and Davies (1990). The Moore and Peltier (1987) mode must rely on a yet unknown mechanism for instability not involving geostrophic dynamics. The conclusion from this paper on the basis of geostrophic dynamics is that for an Eady wave flow, the short-wave instability for uniform potential vorticity cannot account for observed frontal waves; such appear to rely on the existence of a potential vorticity anomaly in the frontal zone. Furthermore, the assumption of uniform potential vorticity implies that the following processes must be small: the β-effect, boundary layer friction, and latent heat release.

It is therefore apparent from this paper and from Joly and Thorpe (1990) that, in general, it is the vertical penetration of the zone of large vorticity due to the presence of a potential vorticity anomaly [or an equivalent thermal anomaly in the generalised sense of

Bretherton (1966)] that is likely to be responsible for the smaller scale frontal wave. Large surface vorticity is not sufficient to produce the observed scales and growth rates although special cases do exist with uniform potential vorticity in which frontal wave modes are produced such as that given by Schär and Davies (1990). Furthermore, it is only when the potential vorticity anomaly has a small horizontal scale that it produces a confined zone of high vorticity. Such an anomaly can arise from the latent heat release in frontal rainbands.

Acknowledgments. Alain Joly would like to acknowledge receipt of Grants by the Programme Atmosphere Météorologique of the Institut National des Sciences de l'Univers of the Centre National de la Recherche Scientifique (CNRS) and from the Royal Society/CNRS under the European Science Exchange Program. Numerical calculations were performed on the CRAY 2 of the GC_2VR in Palaiseau. The code was developed at ECMWF during a long stay in Reading.

APPENDIX

1. The coefficients in the eigenvalue problem

After substitution of the series (12) into the boundary conditions (11), the eigenvalue problem may be written in matrix form as:

$$\lambda \mathbf{Ra} = -\ell \mathbf{Ca}$$

where **R** is a real and **C** is a tri-block-diagonal complex matrix where each blocks are (2×2) matrices. Performing the product $\mathbf{R}^{-1} \times \mathbf{C}$ yields a matrix **D** with the same structure as **C**. The mth block line of **D** is given by:

$$\begin{array}{lccccccc} \text{line } 2M+2m+1 & \beta_{mm-1} & i\gamma_{mm-1} & 0 & 0 & \beta_{mm+1} & -i\gamma_{mm+1} & \\ 2M+2m+2 & i\delta_{mm-1} & \alpha_{mm-1} & 0 & 0 & -i\delta_{mm+1} & \alpha_{mm+1} & \text{(A.1)} \\ \text{row} & 2M+2m-1 & 2M+2m & 2M+2m+1 & 2M+2m+2 & 2M+2m+3 & 2M+2m+4 & \end{array}$$

where

$$\alpha_{mn} = \frac{H_m}{2\cosh\chi_m}\left(\frac{V_2}{H_n}\cosh\chi_n - \frac{V_4}{H_k}\sinh\chi_n\right)$$

$$\beta_{mn} = \frac{H_m}{2\sinh\chi_m}\left(\frac{V_2}{H_n}\sinh\chi_n - \frac{V_4}{H_k}\cosh\chi_n\right)$$

$$\gamma_{mn} = \frac{H_m}{2\sinh\chi_m}\left(\frac{V_1}{H_n}\cosh\chi_n + \frac{V_3}{H_k}\sinh\chi_n\right)$$

$$\delta_{mn} = \frac{H_m}{2\cosh\chi_m}\left(\frac{V_1}{H_n}\sinh\chi_n + \frac{V_3}{H_k}\cosh\chi_n\right). \quad \text{(A.2)}$$

2. The structure of the solution: Vertical velocity

From the series (12), the geostrophic part of the solution $(\Phi', U_g', V_g', \theta')$ is easily obtained. The vertical velocity can be recovered from the thermodynamic equation:

$$\hat{w}' = \frac{g}{\theta_0}\frac{\bar{J}}{\mathcal{N}^2}(\sigma + i\ell\overline{V_g})\hat{\theta} + \frac{g}{\theta_0}\frac{i\ell}{f\mathcal{N}^2}\frac{\partial\bar{\theta}}{\partial X}\hat{\phi}.$$

Introducing the normal mode form, the transformed equations become

$$\frac{1}{\bar{J}}\hat{w} = -\frac{g}{\mathcal{N}^2\theta_0}(\sigma + i\ell\overline{V_g})\hat{\theta} + \frac{g}{\mathcal{N}^2\theta_0}\frac{i\ell}{f}\frac{\partial\bar{\theta}}{\partial X}\hat{\phi}. \quad \text{(A.3)}$$

A crucial difference with quasi-geostrophic theory appears here very clearly: in the latter, we would have a constant buoyancy frequency, N^2, allowing w to be known directly. In the present semi-geostrophic model, the equivalent of this term is now the function of X and Z, $\mathcal{N}^2/\bar{J}$, and implies coupling between harmonics. The ageostrophic circulation in the frontal wave is directly influenced by the degree of frontogenesis reached in the original Eady wave. From the basic state description (3), we can substitute for $1/\bar{J}$, $\overline{V_g}$, and $\partial\bar{\theta}/\partial X$. The equation is then transformed, following the same procedure as on the boundaries. And finally, we substitute for θ_m, θ_{m+1}, ϕ_{m+1}, etc., using their functional expression in Z. For a given level Z, the Fourier coefficients of the vertical velocity are the solution of the following linear system:

$$\begin{aligned} & w_m + \frac{\phi_0 k^2}{2f^2}\left[\left(R\sinh\frac{Z}{H_k} + iI\cosh\frac{Z}{H_k}\right)w_{m+1}\right. \\ & \qquad \left. + \left(R\sinh\frac{Z}{H_k} - iI\cosh\frac{Z}{H_k}\right)w_{m-1}\right] \\ & = -\frac{\sigma}{\mathcal{N}^2}\frac{1}{H_m}\left(A_m\sinh\frac{Z}{H_m} + B_m\cosh\frac{Z}{H_m}\right) \\ & + \frac{\ell}{2}\frac{\phi_0 k}{f\mathcal{N}}\left[\left(\frac{k}{f}\left(R\cosh\frac{Z}{H_k} + iI\sinh\frac{Z}{H_k}\right)\cosh\frac{Z}{H_{m+1}}\right.\right. \\ & \left.\left. - \frac{R\sinh Z/H_k + iI\cosh Z/H_k}{H_{m+1}\mathcal{N}}\sinh\frac{Z}{H_{m+1}}\right)A_{m+1}\right. \\ & + \left(\frac{k}{f}\left(R\cosh\frac{Z}{H_k} + iI\sinh\frac{Z}{H_k}\right)\sinh\frac{Z}{H_{m+1}}\right. \\ & \left.\left. - \frac{R\sinh Z/H_k - iI\cosh Z/H_k}{H_{m+1}\mathcal{N}}\cosh\frac{Z}{H_{m+1}}\right)B_{m+1}\right] \end{aligned}$$

$$+\left(\frac{k}{f}\left(-R\cosh\frac{Z}{H_k}+iI\sinh\frac{Z}{H_k}\right)\cosh\frac{Z}{H_{m-1}}\right.$$
$$\left.+\frac{R\sinh Z/H_k-iI\cosh Z/H_k}{H_{m-1}\mathcal{N}}\sinh\frac{Z}{H_{m-1}}\right)A_{m-1}$$
$$+\left(\frac{k}{f}\left(-R\cosh\frac{Z}{H_k}+iI\sinh\frac{Z}{H_k}\right)\sinh\frac{Z}{H_{m-1}}\right.$$
$$\left.\left.+\frac{R\sinh Z/H_k-iI\cosh Z/H_k}{H_{m-1}\mathcal{N}}\cosh\frac{Z}{H_{m-1}}\right)B_{m-1}\right]. \quad (A.4)$$

For any finite order M, the coefficients $w_m(Z)$ result from this tri-diagonal system, which can be easily solved numerically. Note that the coupling between harmonics becomes stronger as ϕ_0 increases.

REFERENCES

Bjerknes, J., and H. Solberg, 1922: Life cycle of cyclones and the polar front theory of atmospheric circulation. *Geofys. Publikasjoner,* **3**(1), 18 pp.

Bretherton, F. P., 1966: Critical layer instability in baroclinic flows. *Quart. J. Roy. Meteor. Soc.,* **92,** 325–334.

Charney, J. G., 1947: The dynamics of long waves in a baroclinic westerly current. *J. Meteor.,* **4,** 135–162.

Eady, E. T., 1949: Long-waves and cyclone waves. *Tellus,* **1,** 33–52.

Hoskins, B. J., 1975: The geostrophic momentum approximation and the semi-geostrophic equations. *J. Atmos. Sci.,* **32,** 233–242.

——, 1976: Baroclinic waves and frontogenesis. Part I: Introduction and Eady waves. *Quart. J. Roy. Meteor. Soc.,* **102,** 103–122.

——, 1982: The mathematical theory of frontogenesis. *Ann. Rev. Fluid Mech.,* **14,** 131–151.

——, and F. P. Bretherton, 1972: Atmospheric frontogenesis models: Mathematical formulation and solution. *J. Atmos. Sci.,* **29,** 11–37.

——, and N. V. West, 1979: Baroclinic waves and frontogenesis. Part II: Uniform potential vorticity jet flows—cold and warm fronts. *J. Atmos. Sci.,* **36,** 1663–1680.

Joly, A., 1989: Les processus diabatiques et la condensation de l'eau dans les fronts atmosphériques: application à l'étude de leur formation et de leur stabilité. Thèse de doctorat de l'Université Paris VI, Paris, 470 pp.

——, and A. J. Thorpe, 1990: Frontal instability generated by tropospheric potential vorticity anomalies. *Quart. J. Roy. Meteor. Soc.,* **116,** 525–560.

Margules, M., 1905: *Die Energie der Stürm.* Jahrbuch der K.-K. Zentralanstalt für Meteorologie und Erdmagnetismus.

Moore, G. W. K., and W. R. Peltier, 1987: Cyclogenesis in frontal zones. *J. Atmos. Sci.,* **44,** 384–409.

Orlanski, I., 1968: Instability of frontal waves. *J. Atmos. Sci.,* **25,** 178–200.

Schär, C., and H. C. Davies, 1990: An instability of mature cold fronts. *J. Atmos. Sci.,* **47,** 929–950.

Solberg, H., 1928: Integrationen der atmosphärischen Störungsgleichungen. *Geofys. Publ.,* **5**(1), 104–120.

Thorpe, A. J., and K. A. Emanuel, 1985: Frontogenesis in the presence of small stability to slantwise convection. *J. Atmos. Sci.,* **42,** 1809–1824.